Polymerization of Ethylene Molecules Chemisorbed on $CrOH^+$ as a Model System of Chromium-Containing Catalyst

Tetsu Hanmura,[†] Masahiko Ichihashi,[‡] Takashi Monoi,[§] Kazuo Matsuura,[#] and Tamotsu Kondow*[,‡]

East Tokyo Laboratory, Genesis Research Institute, Inc., 717-86 Futamata, Ichikawa, Chiba 272-0001, Japan, Cluster Research Laboratory, Toyota Technological Institute in East Tokyo Laboratory, Genesis Research Institute, Inc., 717-86 Futamata, Ichikawa, Chiba 272-0001, Japan, Research and Development Center, Japan Polyethylene Corporation, 3-1 Chidori-cho, Kawasaki-ku, Kawasaki, Kanagawa 210-0865, Japan, and KM Techno Research, 207-27 Akiba-cho, Totsuka-ku, Yokohama, Kanagawa 245-0052, Japan

Received: November 19, 2004

The reaction process of the production of $CrOH(C_2H_4)_2^+$ was studied in connection with the ethylene polymerization on a silica-supported chromium oxide catalyst (the Phillips catalyst). Cluster ions $CrOH(C_2H_4)_2^+$ and $CrOH(C_4H_8)^+$ were produced by the reactions of $CrOH^+$ with C_2H_4 (ethylene) and C_4H_8 (1-butene), respectively, and were allowed to collide with a Xe atom under single collision conditions. The cross section for dissociation of each parent cluster ion was measured as a function of the collision energy (collision-induced dissociation, or CID). It was found that (i) the CID cross section for the production of $CrOH^+$ from $CrOH(C_2H_4)_2^+$ increases sharply at the threshold energy of 3.16 ± 0.22 eV and (ii) the CID cross section for the production of $CrOH^+$ and C_4H_8 from $CrOH(C_4H_8)^+$ also increases sharply at the threshold energy of 3.26 ± 0.21 eV. In comparison with the calculations based on a B3LYP hybrid density functional method, it is concluded that two ethylene molecules in $CrOH(C_2H_4)_2^+$ are polymerized to become 1-butene. The calculation also shows that the dimerization proceeds via $CrOH(C_2H_4)^+$ (ethylene complex) and $CrOH(C_2H_4)_2^+$ (ethylene complex), in which the ethylene molecules bind with $CrOH^+$ through a π-bonding.

1. Introduction

Ethylene molecules are catalytically polymerized on a silica-supported chromium oxide catalyst that is known as the Phillips catalyst,[1,2] which is used for the production of polyethylene; this method provides more than one-third of the world polyethylene demand.[3] Because of its practical importance, the reaction mechanism of the polymerization on the catalyst has been investigated intensively,[2,4−7] leaving several unsettled issues; for instance, there are the pros and cons on whether the active center for the polymerization is a monatomic[7,8] or a diatomic[9,10] site, etc. In this regard, we have studied reactions of ethylene molecules with cluster ions Cr_n^+ ($n = 1-4$), Cr_nO^+ ($n = 1-4$), and Cr_nOH^+ ($n = 1, 2$) in the gas phase and have revealed that only CrO^+ and $CrOH^+$ adsorb two ethylene molecules on them, under multiple collision conditions.[11] This finding suggests that a Cr atom bonded to an O atom or an OH group on the silica substrate of the Phillips catalyst behaves as the active center for the ethylene polymerization. This inference is verified if one proves that $(C_2H_4)_2$ bonded to CrO^+ and $CrOH^+$ is essentially the same as reaction intermediates that emerge during the course of the polymerization reaction.

In the present experiment, we have measured the dissociation energies of $CrOH(C_2H_4)_2^+$ and $CrOH(C_4H_8)^+$ produced in the reaction of $CrOH^+$ with C_2H_4 (ethylene) and C_4H_8 (1-butene), respectively, by the collision-induced dissociation (CID) method, and we have compared the dissociation energies with those calculated by a density functional method. We conclude that the two ethylene molecules in $CrOH(C_2H_4)_2^+$ are dimerized to become one 1-butene molecule. This result implies that the active center of the Phillips catalyst is actually a Cr atom bonded to an O atom or an OH group of the silica substrate.

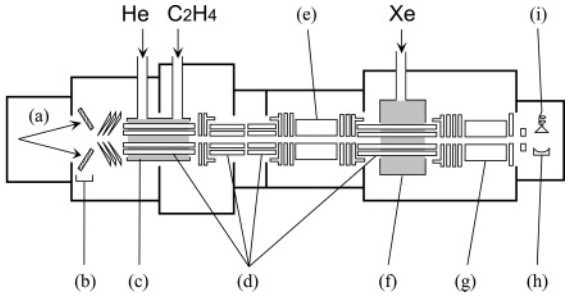

Figure 1. Schematic drawing of the apparatus used in the present study. Legend is as follows: (a) argon-ion beam, (b) chromium targets, (c) cooling cell, (d) octopole ion guides, (e) first quadrupole mass filter, (f) collision cell, (g) second quadrupole mass filter, (h) ion conversion dynode, and (i) secondary electron multiplier.

2. Experimental Section

Figure 1 shows a schematic drawing of the apparatus used in the measurements of cross sections for CID. A brief description is given here, except for the modification made for the present study, because the detailed description has been reported previously.[12,13] The apparatus consists of a cluster ion source, a cooling cell, quadrupole mass filters, a collision cell, and a detector, which are connected to each other by octopole ion guides.

* Corresponding author. E-mail: kondow@clusterlab.jp.
† East Tokyo Laboratory, Genesis Research Institute, Inc.
‡ Cluster Research Laboratory, Toyota Technological Institute.
§ Research and Development Center, Japan Polyethylene Corporation.
# KM Techno Research.

10.1021/jp040723v CCC: $30.25
Published on Web 07/06/2005

An argon-ion beam from a plasma ion source (CORDIS Ar25/35c, Rokion Ionenstahl-Technologie) at an acceleration energy of 15 keV was separated into four ion beams, each of which was allowed to bombard one out of four separate chromium targets mounted circularly around the center axis of the plasma ion source. Oxide and hydroxide ions of chromium were produced without the introduction of any additional gas; these ions were likely to be produced by reactions with a trace amount of residual gases such as water. All the ions thus produced were admitted into an octopole ion guide that was mounted inside a cooling cell surrounded with a jacket. The cooling cell was filled with a mixture of helium and ethylene gases with a 20:1 molar ratio at a total pressure of $>10^{-3}$ Torr. In the cooling cell, the ions were cooled to 77 and 300 K with and without liquid nitrogen in the jacket, respectively. The collision frequency of $CrOH^+$ with He atoms is much higher than that with C_2H_4, so that $CrOH(C_2H_4)_2^+$ attains a thermal equilibrium with the helium gas. Only $CrOH(C_2H_4)_2^+$ produced in the cooling cell was allowed to pass through the first quadrupole mass filter for the measurement of the CID in an octopole ion guide that was surrounded by a collision cell containing xenon gas at a pressure of $\sim 6 \times 10^{-5}$ Torr. At this pressure, a single collision condition was fulfilled. The pressure in the collision cell was monitored by a spinning rotor gauge (MKS, model SRG-2). The collision energy was varied by changing a DC voltage that was applied to the octopole ion guide. The product and the intact parent ions from the collision cell were mass-analyzed in the second quadrupole mass filter and were detected by an ion conversion dynode, followed by a secondary electron multiplier (Murata Ceratron, model EMS-6081B). The spread of the translational energy of $CrOH(C_2H_4)_2^+$ was measured by applying a retarding voltage to the octopole ion guide that was mounted in the collision cell, and the energy spread was determined to be typically 2 eV in the laboratory frame. In the collision of $CrOH(C_2H_4)_2^+$ with a xenon atom, this energy spread amounts to ± 0.5 eV in the center-of-mass frame. This collision energy spread was taken into account in determining the dissociation energy (see Section 4.A). In addition, $CrOH(C_4H_8)^+$ was produced in the reaction of $CrOH^+$ with 1-butene in the presence of the helium gas in the cooling cell for the measurement of the CID cross sections. Note that the temperature of the cooling cell and the gas inlet was maintained at 300 K, to prevent the 1-butene gas from condensing inside the cooling cell and the inlet tube.

The total CID cross section (σ_r) is calculated as

$$\sigma_r = \frac{k_B T}{Pl} \ln\left(\frac{I_r + \sum I_p}{I_r}\right) \quad (1)$$

where I_r and $\sum I_p$ represent the intensity of the intact parent ion and the sum of the intensities of the product ions, respectively; P and T are the pressure and the temperature of the xenon gas, respectively; l is the effective path length of the collision region ($l = 120$ mm), and k_B is the Boltzmann constant. The partial cross section (σ_p) for the formation of a given product ion is given as

$$\sigma_p = \sigma_r \frac{I_p}{\sum I_p} \quad (2)$$

where $I_p/\sum I_p$ represents the branching fraction for the product ion. The uncertainties in the cross sections consist of (i) systematic errors that result from the uncertainties in the ion collection efficiency and in determining the pressure P and the effective path length l, and (ii) statistical errors that result from the fluctuation of the ion intensity. The systematic and statistical errors are typically 30% and 20%, respectively. The systematic errors can be ruled out from the argument in cases when the collision-energy dependence of the CID cross sections is discussed in a relative manner.

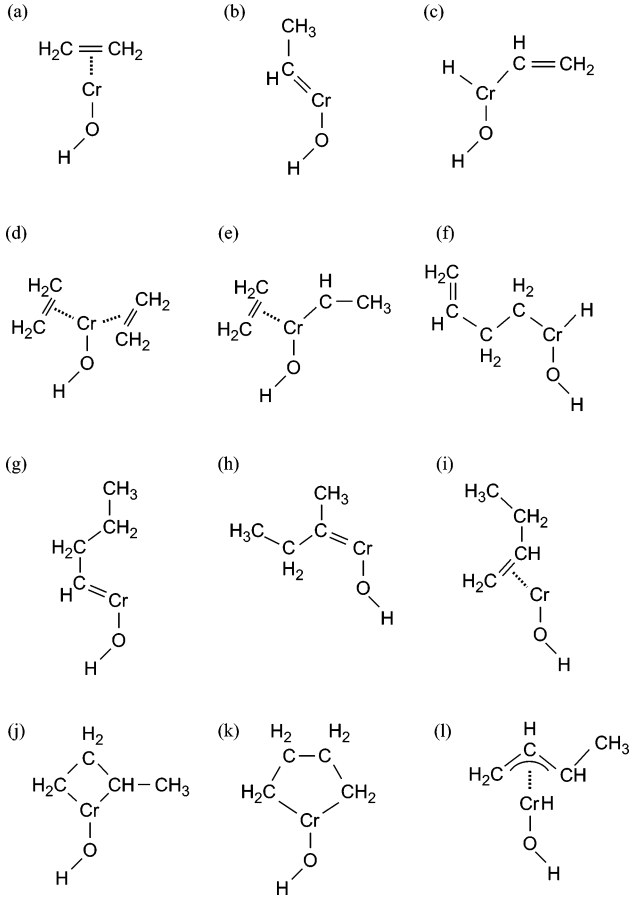

Figure 2. Initial geometries of $CrOH(C_2H_4)^+$ and $CrOH(C_2H_4)_2^+$ used in the present calculation with the spin multiplicity of $M = 5$. Geometries in Figure 2a−c show the geometries of $CrOH(C_2H_4)^+$: (a) an ethylene complex, (b) an ethylidene complex, and (c) a vinyl complex. Geometries in Figure 2d−l show the geometries of $CrOH(C_2H_4)_2^+$: (d) an ethylene complex, (e) an ethylene−ethylidene complex, (f) a butenyl complex, (g and h) butylidene complexes, (i) a 1-butene complex, (j and k) metallacycle complexes, and (l) a π-allyl complex.

3. Computational Procedure

All the optimized geometries with given spin multiplicities were computed with the Gaussian 98W program,[14] using the B3LYP hybrid density functional method, namely, Becke's gradient-corrected exchange-correlation density functionals,[15] combined with Lee, Yang, and Parr's nonlocal correlation.[16] Initially, a geometry optimization was performed using LANL2DZ (Los Alamos National Laboratory second Double-Zeta) basis sets[17] for Cr, 6-31G(d) for C and O, 6-31G for H in the ethylene molecule, and 6-31(d,p) for H in the OH group, respectively. The initial geometries for the optimization were constructed from plausible structures of the reaction products and intermediates shown in Figure 2 (see Section 4.B) with varying bond lengths and bond angles. After the geometry optimization, a single-point calculation was made for energy estimation of the optimized geometry using larger basis sets, that is, LANL2DZ basis sets with an option of an f-polarization function[18] that has

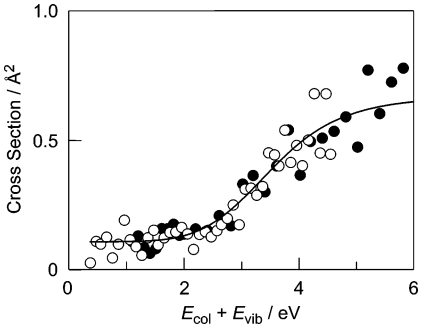

Figure 3. Cross sections for the collision-induced dissociation (CID) of $CrOH(C_2H_4)_2^+$ to $CrOH^+$, as a function of the total energy, which is the sum of the collision energy, E_{col}, and the initial vibrational energy, E_{vib}, of $CrOH(C_2H_4)_2^+$. The open and closed circles represent the cross sections for $CrOH(C_2H_4)_2^+$ with internal temperatures of 77 and 300 K, respectively. The solid line shows the best-fit cross sections with a threshold energy of 3.16 eV (see text).

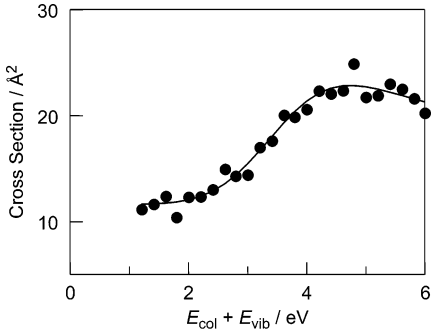

Figure 4. Cross sections for the CID of $CrOH(C_4H_8)^+$ (1-butene complex) with an internal temperature of 300 K to $CrOH^+$ and C_4H_8, as a function of the total energy, which is the sum of the collision energy E_{col} and the initial vibrational energy E_{vib} of $CrOH(C_4H_8)^+$. The solid line shows the best-fit cross sections with the threshold energy of 3.26 eV (see text).

an exponent of 1.941 for Cr, 6-311G(d) for C, 6-311+G(d) for O, and 6-311G(d,p) for H.

4. Results

4.A. Collision-Induced Dissociation. *4.A.1. Dissociation Processes Induced by Collision.* In the CID of $CrOH(C_2H_4)_2^+$, which was prepared via the reaction of $CrOH^+$ with C_2H_4, $CrOH(C_2H_4)^+$ and $CrOH^+$ were produced as the fragment ions. The counter neutral product to $CrOH(C_2H_4)^+$ should be C_2H_4, based on the energetics, whereas the counter neutral product to $CrOH^+$ is either $2C_2H_4$ (ethylene) or C_4H_8 (probably 1-butene). Therefore, the following reaction processes are conceivable:

$$CrOH(C_2H_4)_2^+ \rightarrow CrOH(C_2H_4)^+ + C_2H_4 \qquad (3)$$

$$CrOH(C_2H_4)_2^+ \rightarrow CrOH^+ + 2C_2H_4/C_4H_8 \qquad (4)$$

4.A.2. Determination of Threshold Energies for Dissociation. Figure 3 shows the cross sections for the dissociation of $CrOH(C_2H_4)_2^+$ that has internal temperatures of 77 and 300 K into $CrOH^+$ in collision with a Xe atom, as a function of the total energy, which is the sum of the collision energy (E_{col}) and the initial vibrational energy (E_{vib}) of the parent ion. The vibration energy is given as $E_{vib} = 3(m - 6)k_BT$, where m represents the number of atoms in the parent ion, k_B is the Boltzmann constant, and T is the internal temperature of the incoming parent ion.

The threshold energy (E_0) was derived from the collision-energy (E_{col}) dependence of the CID cross section (σ) in the vicinity of the threshold energy region, using the semiempirical equation[19]

$$\sigma = \sigma_0 \frac{(E_{vib} + E_{col} - E_0)^N}{E_{col}} \qquad (5)$$

where σ_0 is an energy-independent scaling factor. The exponent (N) was treated as an adjustable parameter, although it is given theoretically for particular types of reactions.[20−23] In the present analysis, eq 5 was modified to introduce the effects of the thermal motion of the Xe atom and the energy spread in the translational energy of the parent ion, as given by Chantry[24] and Lifshitz et al.,[25] respectively. The solid curve in Figure 3 shows the best-fit one obtained by the least-squares fitting, leaving E_0, σ_0, and N as the adjustable parameters. In the fitting procedure, a constant offset was introduced by considering the fact that a small portion of the parent ions is represented by ions with more weakly bound ethylene molecules. As shown in Figure 3, the measured CID cross sections agree with the calculated cross sections, with the threshold energy being $E_0 = 3.16 \pm 0.22$ eV.

4.A.3. Threshold Energy for Dissociation of $CrOH(C_4H_8)^+$. As described in Section 2, a parent ion adsorbed with one 1-butene molecule, $CrOH(C_4H_8)^+$, was prepared and dissociated in collision with a Xe atom. The mass spectrum of the product ion shows that the CID proceeds as follows:

$$CrOH(C_4H_8)^+ \rightarrow CrOH^+ + C_4H_8 \qquad (6)$$

Figure 4 shows the CID cross section for reaction 6, plotted against $E_{vib} + E_{col}$. The threshold energy for the production of $CrOH^+$ from $CrOH(C_4H_8)^+$ was determined to be 3.26 ± 0.21 eV by following the same procedure used in the analysis of $CrOH(C_2H_4)_2^+$. The presence of the large offset in the energy region lower than the threshold energy implies that there is a significant amount of $CrOH(C_4H_8)^+$ in which C_4H_8 is weakly bound to $CrOH^+$.

4.B. Structures and Energies of Reaction Intermediates and Products. *4.B.1. Reliability of the Present Calculation.* The reliability of the present calculation was examined by comparing the optimized geometry of $CrOH^+$ for different spin multiplicities (given as $M = 2S + 1$), and the bond energy of $Cr^+-C_2H_4$ obtained in the present calculation with those obtained by other groups. The ground state of $CrOH^+$ was found to have $M = 5$ with Cr−O and O−H bond lengths of 1.77 and 0.97 Å, respectively, and a Cr−O−H bond angle of 138.6°. In the ab initio molecular orbital calculation of an MP2 (full) level by Glusker and co-workers,[26] $CrOH^+$ has the $^5A'$ ground state with Cr−O and O−H bond lengths of 1.745 and 0.964 Å, respectively, and a Cr−O−H bond angle of 134.3°. As described previously, the present calculation reproduces the results of the ab initio calculation reasonably well.

On the other hand, the present calculation showed that the ground state of $Cr(C_2H_4)^+$ has $M = 6$ and the bond energy of $Cr^+-C_2H_4$ is 1.22 eV, whereas Bauschlichter et al. have shown by their ab initio calculation that the $Cr^+-C_2H_4$ bond energy of $Cr(C_2H_4)^+$ in the $^6A_1$ ground state is 1.13 eV.[27] The two different calculations give almost the same bond energy, which is slightly higher than the $Cr^+-C_2H_4$ bond energy of 0.99 ± 0.11 eV measured experimentally by Armentrout and co-workers.[28]

4.B.2. $CrOH(C_2H_4)^+$. By considering the spin conservation, the optimized geometries of $CrOH(C_2H_4)^+$ with the spin multiplicity of $M = 5$ were computed because $CrOH^+$ in the ground state has $M = 5$, as described previously, and C_2H_4 in

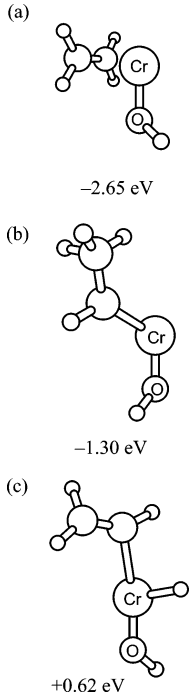

Figure 5. Optimized geometries of $CrOH(C_2H_4)^+$: (a) the ethylene complex, (b) the ethylidene complex, and (c) the vinyl complex. Energies are shown with respect to $CrOH^+ + C_2H_4$.

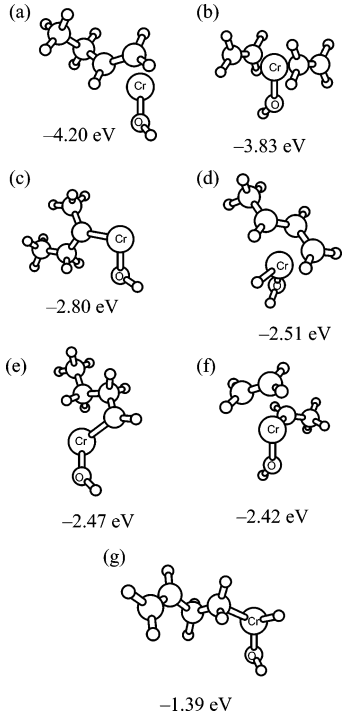

Figure 6. Optimized geometries of $CrOH(C_2H_4)_2^+$: (a) the 1-butene complex, (b) the ethylene complex, (c) the *sec*-butylidene complex, (d) the π-allyl complex, (e) the butylidene complex, (f) the ethylene−ethylidene complex, and (g) the butenyl complex. Energies are shown with respect to $CrOH^+ + 2C_2H_4$.

the ground state has $M = 1$. The initial geometries used for the geometry optimization are shown in Figure 2a, b, and c, which are called an "ethylene complex", an "ethylidene complex", and a "vinyl complex", respectively: an ethylene molecule is bonded molecularly to the Cr atom through a π-bond in the ethylene complex, bonded as $=CHCH_3$ (ethylidene) by forming a Cr=C double bond in the ethylidene complex, and dissociatively bonded as $-CH=CH_2$ (vinyl group) and H on the Cr atom in the vinyl complex. These geometries were chosen because similar species are said to be formed in the initiation step of the ethylene polymerization on supported chromium oxide catalysts.[8,29]

Figure 5 shows the optimized geometries and their energies, with respect to the energy of $CrOH^+ + C_2H_4$; these energies are equal to the bond energies of C_2H_4 on $CrOH^+$. The ethylene complex (the geometry shown in Figure 5a) was found to be the most stable, whereas the ethylidene complex (the geometry shown in Figure 5b) is 1.35 eV less stable than the ethylene complex. The vinyl complex (the geometry shown in Figure 5c) is less stable than $CrOH^+ + C_2H_4$, and, therefore, it is unlikely that the ethylene molecule is dissociatively bound on $CrOH^+$ in $CrOH(C_2H_4)^+$.

4.B.3. $CrOH(C_2H_4)_2^+$. The geometry optimization for $CrOH(C_2H_4)_2^+$ was performed for $M = 5$ by taking the spin conservation into consideration. Initial geometries for the optimization of $CrOH(C_2H_4)_2^+$ are shown in Figure 2d−l. In Figure 2, the geometry shown in Figure 2d shows an ethylene complex, in which two ethylene molecules are separately attached to the Cr atom by forming π-bonds; the geometry shown in Figure 2e shows an "ethylene−ethylidene complex", in which one molecular ethylene and one ethylidene moiety are attached to the Cr atom; the geometry shown in Figure 2f shows a "butenyl complex"; the geometries shown in Figure 2g and h show two conformers of "butylidene complexes"; and the geometry shown in Figure 2i shows a "butene complex". The geometries shown in Figure 2j and k exhibit "metallacycle complexes", and the geometry shown in Figure 2l shows a "π-allyl complex". These geometries are selected because they are akin to the reaction intermediates emerging in the ethylene polymerization on silica-supported chromium oxide catalysts.[2,8,30]

Figure 6 shows the geometries optimized from these initial geometries. The energy value given below each geometry is the total energy, with respect to that of $CrOH^+ + 2C_2H_4$. The geometry shown in Figure 6a illustrates the 1-butene complex, in which one 1-butene molecule is bound to the Cr atom by a π-bond. This 1-butene complex is energetically the most stable. The ethylene complex (the geometry shown in Figure 6b), in which two ethylene molecules attach separately to $CrOH^+$, has a total energy that is 0.37 eV higher than that of the 1-butene complex. The butylidene complexes (the geometries shown in Figure 6c and e), the π-allyl complex (the geometry shown in Figure 6d), the ethylene−ethylidene complex (the geometry shown in Figure 6f), and the butenyl complex (the geometry shown in Figure 6g) are less stable. Both of the initial geometries given by the geometries exhibited in Figure 2e and j were converged to the same ethylene−ethylidene complex with the geometry shown in Figure 6f. No optimized geometry was obtained from the metallacycle complex with the geometry shown in Figure 2k. In summary, the 1-butene complex and the ethylene complex were obtained to be the most plausible products in the reaction of $CrOH^+$ with $2C_2H_4$.

The dissociation energies of the two most stable species, the 1-butene complex (see Figure 6a) and the ethylene complex (see Figure 6b), were calculated to be 3.19 and 3.83 eV, with respect to $CrOH^+ + C_4H_8$ and $CrOH^+ + 2C_2H_4$, respectively.

5. Discussion

5.A. Dissociation Energy of the 1-Butene Complex. The dissociation energy of $CrOH(C_4H_8)^+$, produced by the reaction of $CrOH^+$ with C_4H_8 (1-butene), was determined to be 3.26 ±

0.21 eV by the CID measurement, as described in Section 4.A. On the other hand, the density functional calculation gives the dissociation energy of 3.19 eV for the 1-butene complex. The agreement between the experimental and the theoretical dissociation energies leads us to conclude that $CrOH(C_4H_8)^+$ produced from $CrOH^+$ and 1-butene is the 1-butene complex.

5.B. Identification of Ethylene-Adsorbed Parent Ion. As described previously, the dissociation energy of the 1-butene complex $CrOH(C_4H_8)^+$ into $CrOH^+ + C_4H_8$ was obtained experimentally and theoretically to be 3.26 ± 0.21 and 3.19 eV, respectively. These values agree well with the measured dissociation energy of 3.16 ± 0.22 eV for $CrOH(C_2H_4)_2^+$ to produce $CrOH^+$. The agreement supports the belief that the parent ion, $CrOH(C_2H_4)_2^+$, produced by the reaction of $CrOH^+$ with $2C_2H_4$ is indeed the 1-butene complex, in which the two ethylene molecules react to become one 1-butene molecule. Otherwise, the parent ion should be the ethylene complex with an energy of 3.83 eV for dissociation into $CrOH^+$ and $2C_2H_4$. However, the measured dissociation energy (3.16 ± 0.22 eV) is much lower than that of the ethylene complex calculated. Therefore, it is concluded that the two adsorbed ethylene molecules on $CrOH^+$ are polymerized to become 1-butene.

5.C. Intermediate Species in Dimerization. It is conceivable that ethylene molecules react consecutively with $CrOH^+$ to become $CrOH(C_2H_4)_2^+$ via $CrOH(C_2H_4)^+$, which is likely to be the most stable ethylene complex (see Figure 5). The freshly prepared $CrOH(C_2H_4)_2^+$ should be the ethylene complex, because the intermediate species, $CrOH(C_2H_4)^+$, also is the ethylene complex. It follows that the two ethylene molecules attached to $CrOH^+$ (the freshly prepared ethylene complex, $CrOH(C_2H_4)_2^+$) are polymerized to become 1-butene attached to $CrOH^+$ as the final product, which was determined to be the 1-butene complex. The carbene complexes (the geometries shown in Figure 6c, e, and f) are proved to be the reaction intermediates by the present calculation, on the premise that there is no appreciable energy barrier among the reaction intermediates on the reaction potential, where the energy barrier was not calculated because the present calculation is not good enough to address the transition state along the reaction potential from the ethylene complex to the 1-butene complex. Note that the reaction intermediates of the ethylene polymerization on the Phillips catalyst are proposed to be the carbene and the metallacycle complexes[8,29,30] as well. Consulting with the polymerization on the Phillips catalyst,[29] one constructs the reaction path of the ethylene dimerization on $CrOH^+$ as follows. Two ethylene molecules are adsorbed on $CrOH^+$ as an ethylene π-complex (see Figure 6b), which changes into an ethylene−ethylidene complex (see Figure 6f). The ethylene−ethylidene complex is polymerized to become a butylidene complex (see Figure 6e) probably via a metallacycle species that has the geometries shown in Figure 2j or k, although the present calculation does not prove the existence of the metallacycle species. Finally, the butylidene complex changes to a 1-butene complex (see Figure 6a).

5.D. Active Center of the Phillips Catalyst. Let us compare characteristic electronic structures of an isolated $CrOH^+$ and Cr/SiO_2 systems[31−33] mimicked from the Phillips catalyst, in terms of their catalytic activity. The charge on the Cr site in $CrOH^+$ was calculated to be +1.4 in the present calculation, using the Mulliken charge analysis, whereas those in the Cr/SiO_2 systems have been reported to be between +1.0 and +1.7, where the net charges in the Cr/SiO_2 systems are maintained to be zero.[31] The 4s electron of the Cr site in the $CrOH^+$ is absent because the electron is depleted in forming the positive charge. The depletion of the 4s electron in the $CrOH^+$ does not matter much when one compares catalytic reactions of ethylene molecules on the $CrOH^+$ with those on the Cr/SiO_2 systems, because their 3d electrons have a central role in the catalytic reactions, and it has been found that the diffuse 4s electron in the Cr site of the Cr/SiO_2 system is used for bonding formation with the Si sites (3s orbital) of the SiO_2.[32] Actually, the present calculation shows that the Cr−ethylene bonding orbitals in the ethylene complexes (see Figures 5a and 6b) are mainly composed of 3d orbitals of Cr and 2p orbitals of C.

In addition to the issue of the electronic structure, one should consider the difference in the geometric constraints when the reaction intermediates (such as the Cr−ethylene complexes) are formed on $CrOH^+$ and on the Cr/SiO_2 systems. The Cr−ethylene complexes have been proved to be formed readily, regardless of the geometries the Cr/SiO_2 systems take.[31,33] Similar Cr−ethylene complexes are formed readily on the $CrOH^+$ without any argument. In conclusion, the isolated $CrOH^+$ is an appropriate model representing the Cr/SiO_2 system, that is, the surface of the Phillips catalyst.

The arguments given previously lead us to conclude that the initial step of the ethylene polymerization on the Phillips catalyst can be mimicked by the dimerization of the ethylene molecules on $CrOH^+$ and, hence, a Cr atom bonded to an O atom or an OH group of the silica substrate works as an active center for the ethylene polymerization.

6. Conclusion

In the present study, we measured and calculated the dissociation energies of the ionic species produced by the reaction of $CrOH^+$ with ethylene and 1-butene, and revealed that the ionic species produced by the reaction of $CrOH^+$ with two ethylene molecules is the 1-butene complex, in which one 1-butene molecule is bound to $CrOH^+$. This finding leads us to conclude that two ethylene molecules are polymerized to become 1-butene on $CrOH^+$. Applying this finding to the catalytic polymerization on the Phillips catalyst (silica-supported chromium oxide catalyst), one concludes that the active center for the ethylene polymerization on the Phillips catalyst is a Cr atom bound to an O atom or an OH group on the silica substrate.

Acknowledgment. The authors are grateful to Professor Shigeyoshi Sakaki for his advice on the density functional theory calculation used in the present study. This work was supported by the Special Cluster Research Project of Genesis Research Institute, Inc.

References and Notes

(1) Hogan, J. P.; Banks, R. L. Belgium Patent No. 530617, 1955.
(2) McDaniel, M. P. *Adv. Catal.* **1985**, *33*, 47.
(3) Weckhuysen, B. M.; Schoonheydt, R. A. *Catal. Today* **1999**, *51*, 215.
(4) Marsden, C. E. *Plast., Rubber Compos. Process. Appl.* **1994**, *21*, 193.
(5) Wechhuysen, B. M.; Wachs, I. E.; Schoonheydt, R. A. *Chem. Rev.* **1996**, *96*, 3327.
(6) McDaniel, M. P. *Ind. Eng. Chem. Res.* **1988**, *27*, 1559.
(7) Hogan. J. P. In *Applied Industrial Catalysis*; Leach, B. E., Ed.; Academic Press: New York, 1983; Vol. 1, p 149.
(8) Krauss, H. L.; Hums, E. *Z. Naturforsch., B: Anorg. Chem., Org. Chem.* **1979**, *34B*, 1628.
(9) Rebenstorf, B.; Larsson, R. *J. Mol. Catal.* **1981**, *11*, 247.
(10) Rebenstorf, B. *J. Mol. Catal.* **1989**, *56*, 170.
(11) Hanmura, T.; Ichihashi, M.; Monoi, T.; Matsuura, K.; Kondow, T. *J. Phys. Chem. A* **2004**, *108*, 10434.
(12) Hirokawa, J.; Ichihashi, M.; Nonose, S.; Tahara, T.; Nagata, T.; Kondow, T. *J. Chem. Phys.* **1994**, *101*, 6625.

(13) Ichihashi, M.; Hanmura, T.; Yadav, R. T.; Kondow, T. *J. Phys. Chem. A* **2000**, *104*, 11885.
(14) Frisch, M. J.; Trucks, G. W.; Schlegel, H. B.; Scuseria, G. E.; Robb, M. A.; Cheeseman, J. R.; Zakrzewski, V. G.; Montgomery, J. A., Jr.; Stratmann, R. E.; Burant, J. C.; Dapprich, S.; Millam, J. M.; Daniels, A. D.; Kudin, K. N.; Strain, M. C.; Farkas, O.; Tomasi, J.; Barone, V.; Cossi, M.; Cammi, R.; Mennucci, B.; Pomelli, C.; Adamo, C.; Clifford, S.; Ochterski, J.; Petersson, G. A.; Ayala, P. Y.; Cui, Q.; Morokuma, K.; Malick, D. K.; Rabuck, A. D.; Raghavachari, K.; Foresman, J. B.; Cioslowski, J.; Ortiz, J. V.; Baboul, A. G.; Stefanov, B. B.; Liu, G.; Liashenko, A.; Piskorz, P.; Komaromi, I.; Gomperts, R.; Martin, R. L.; Fox, D. J.; Keith, T.; Al-Laham, M. A.; Peng, C. Y.; Nanayakkara, A.; Gonzalez, C.; Challacombe, M.; Gill, P. M. W.; Johnson, B. G.; Chen, W.; Wong, M. W.; Andres, J. L.; Gonzalez, C.; Head-Gordon, M.; Replogle, E. S.; Pople, J. A. *Gaussian 98*, revision A.7; Gaussian, Inc.: Pittsburgh, PA, 1998.
(15) Becke, A. D. *J. Chem. Phys.* **1993**, *98*, 5648.
(16) Lee, C.; Yang, W.; Parr, R. G. *Phys. Rev. B* **1988**, *37*, 785.
(17) Hay, P. J.; Wadt, W. R. *J. Chem. Phys.* **1985**, *82*, 270.
(18) Ehlers, A. W.; Böhme, M.; Dapprich, S.; Gobbi, A.; Höllwarth, A.; Jonas, V.; Köhler, K. F.; Stegmann, R.; Veldkamp, A.; Frenking, G. *Chem. Phys. Lett*. **1993**, *208*, 111.
(19) Armentrout, P. B. *Int. J. Mass Spectrom.* **2000**, *200*, 219.
(20) Levine, R. D.; Bernstein, R. B. *Chem. Phys. Lett.* **1971**, *11*, 552.
(21) Rebick, C.; Levine, R. D. *J. Chem. Phys.* **1973**, *58*, 3942.
(22) Eu, B. C.; Liu, W. S. *J. Chem. Phys.* **1975**, *63*, 592.
(23) Chesnavich, W. J.; Bowers, M. T. *J. Phys. Chem.* **1979**, *83*, 900.
(24) Chantry, P. J. *J. Chem. Phys.* **1971**, *55*, 2746.
(25) Lifshitz, C.; Wu, R. L. C.; Tiernan, T. O.; Terwilliger, D. T. *J. Chem. Phys.* **1978**, *68*, 247.
(26) Trachtman, M.; Markham, G. D.; Glusker, J. P.; George, P.; Bock, C. W. *Inorg. Chem.* **2001**, *4*0, 4230.
(27) Bauschlichter, C. W., Jr.; Langhoff, S. R.; Partridge, H. In *Organometallic Ion Chemistry*; Freiser, B. S., Ed.; Kluwer: Dordrecht, The Netherlands, 1996; pp 47−87.
(28) Sievers, M. R.; Jarvis, L. M.; Armentrout, P. B. *J. Am. Chem. Soc.* **1998**, *120*, 1891.
(29) Kantcheva, M.; Dalla Lana, I. G.; Szymura, J. A. *J. Catal.* **1995**, *154*, 329.
(30) Ghiotti, G.; Garrone, E.; Zecchina, A. *J. Mol. Catal.* **1988**, *46*, 61.
(31) Espelid, Ø.; Børve, K. J. *J. Catal.* **2000**, *195*, 125.
(32) Ma, Q.; Klier, K.; Cheng, H.; Mitchell, W. *J. Phys. Chem. B* **2002**, *106*, 10121.
(33) Espelid, Ø; Børve, K. J. *J. Catal.* **2002**, *205*, 366.